High heat flux testing of newly developed tungsten components for WEST

G. Pintsuk, M. Missirlian, G.-N. Luo, Q. Li, W. Wang, D. Guilhem, J. Bucalossi

▶ **To cite this version:**

G. Pintsuk, M. Missirlian, G.-N. Luo, Q. Li, W. Wang, et al.. High heat flux testing of newly developed tungsten components for WEST. Fusion Engineering and Design, 2021, 173, pp.112835. 10.1016/j.fusengdes.2021.112835 . cea-04746703

HAL Id: cea-04746703
https://cea.hal.science/cea-04746703v1

Submitted on 21 Oct 2024

HAL is a multi-disciplinary open access archive for the deposit and dissemination of scientific research documents, whether they are published or not. The documents may come from teaching and research institutions in France or abroad, or from public or private research centers.

L'archive ouverte pluridisciplinaire **HAL**, est destinée au dépôt et à la diffusion de documents scientifiques de niveau recherche, publiés ou non, émanant des établissements d'enseignement et de recherche français ou étrangers, des laboratoires publics ou privés.

Fusion Engineering and Design 173 (2021) 112835

Contents lists available at ScienceDirect

Fusion Engineering and Design

journal homepage: www.elsevier.com/locate/fusengdes

High heat flux testing of newly developed tungsten components for WEST

G. Pintsuk [a,*], M. Missirlian [b], G.-N. Luo, Resources [c], Q. Li, Resources [c], W. Wang, Resources [c], D. Guilhem [b], J. Bucalossi, Funding acquisition [b]

[a] Forschungszentrum Jülich GmbH, Institut für Energie- und Klimaforschung – Plasmaphysik, Partner of the Trilateral Euregio Cluster (TEC), 52425 Jülich, Germany
[b] CEA, IRFM, F-13108 Saint-Paul-Lez-Durance, France
[c] Institute of Plasma Physics, Chinese Academy of Sciences (ASIPP), Hefei, Anhui, China

ARTICLE INFO

Keywords:
WEST
Tungsten divertor
High heat flux

ABSTRACT

In preparation of the production of the actively cooled tungsten targets for the lower divertor of WEST (W -for tungsten- Environment in Steady-state Tokamak), the qualification of suppliers is done by exposing small-scale mock-ups to cyclic high heat flux tests in the electron beam facility JUDITH 1 at Forschungszentrum Jülich. Thereby, the small-scale mock-ups are based on the ITER design, consisting of 7 monoblocks mounted on a CuCrZr cooling tube and connected via a soft Cu-interlayer.

The results presented herein focus on the high heat flux test results of two mock-ups produced by AT&M in China. The testing was performed by thermal cycling at 10 MW/m^2 and 20 MW/m^2 with a maximum of 1200 cycles at 10 MW/m^2 followed by 500 cycles at 20 MW/m^2 without obvious damage formation.

The qualification is supported by subsequent hardness tests and microstructural analyses. The latter focus on local variation of tungsten recrystallization and macro-crack formation and deformation induced changes in the heat sink materials.

1. Introduction

The WEST (W -for tungsten- Environment in Steady-state Tokamak) project is based on an upgrade of Tore Supra tokamak. ITER-like actively cooled tungsten targets (monoblocks) will be integrated in the lower divertor and a new set of actively cooled tungsten coated plasma facing components will cover a part of the vessel to provide a fully metallic environment [1–3].

In preparation of the production of the actively cooled tungsten targets for the lower divertor the qualification of suppliers is done by exposing small-scale mock-ups to cyclic high heat flux tests in the electron beam facility JUDITH 1 at Forschungszentrum Jülich [4]. Thereby, the small-scale mock-ups are based on the ITER design [5,6], consisting of 7 monoblocks mounted on a CuCrZr cooling tube and connected via a soft Cu-interlayer. The tests performed provide information on the thermal fatigue response of the mock-ups and in particular the interface quality of the dissimilar joints in the component (W/CuCrZr with a soft and thin Cu interlayer), which is the primary focus of this qualification campaign that is set-up in a similar way as those performed for ITER [7]. In addition, due to the characteristics of the electron beam also conclusions on the synergistic effects of transient and steady state thermal loads can be drawn while investigating surface effects is not the primary aim of this study. Accordingly and although relevant for the understanding of the behavior of tungsten in general under fusion relevant operational conditions, the combination of thermal loads with plasma specific loads related to the application of hydrogen species, helium and/or impurities resulting in surface morphology changes are not addressed here as this was the case in [8,9] by stepwise exposure in different facilities.

The results presented herein focus on the high heat flux test results of two mock-ups produced by AT&M in China. The testing was performed by thermal cycling at 10 MW/m^2 and at 20 MW/m^2 in correlation but not 100% identical in terms of the number of applied cycles to qualification procedures applied for ITER divertor components [7].

The discussion of the results comprises the thermal performance of the mock-ups during thermal cycling as well as the subsequent microstructural analyses. The latter focus on the most important issues determined in earlier studies on ITER qualification mock-ups and components, i.e. tungsten recrystallization and macro-crack formation, the integrity of the CuCrZr cooling tube, and plastic deformation induced changes in the pure Cu-interlayer [10-13].

* Corresponding author.
E-mail addresses: g.pintsuk@fz-juelich.de, irstname.lastname@some.mail.server (G. Pintsuk).

https://doi.org/10.1016/j.fusengdes.2021.112835
Received 18 May 2021; Received in revised form 26 July 2021; Accepted 3 August 2021
Available online 24 August 2021
0920-3796/© 2021 Published by Elsevier B.V.

2. Manufacturing, testing and characterization

2.1. Component manufacturing

Both tested components (M-1_2 and M-2_2 – see Fig. 1) were produced by AT&M, China, and consist of 7 W-monoblock tiles (28 × 28 × 12 mm^3, 17 mm diameter hole, 6 mm thickness on plasma facing side). These were made from warm rolled (~1100°C) W-plates with a purity of ~99.95% and a tensile strength at 1000°C of ~470 MPa in rolling direction. On the inner tube wall a pure OF-Cu interlayer with a thickness of 1 mm was HIPed in a first process step for each block individually. This was followed by a second step HIP cycle joining Cu and the inserted CuCrZr cooling tube with a wall thickness of 1.5 mm and an inner diameter of 12 mm using ring shaped W-spacers between the different W-blocks. For enhancing the heat removal capacity, a swirl tape with a twist ratio of 2 was inserted into the cooling tube.

2.2. High heat flux testing

The high heat flux testing was performed with the electron beam facility JUDITH 1 at Forschungszentrum Jülich. The beam width at full width half maximum was 1 mm and the scanning frequency for both, x- and y-direction, was in the range of 30 to 50 kHz and chosen in such a way that a homogeneous loading profile is achieved using a triangular scanning mode.

The cooling conditions using water at an inlet temperature of 22-24°C were set to a water velocity of ~10 m/s in the cooling tube of the mock-up resulting in an inlet water pressure of ~2.25 MPa. This is due to the linear relationship between feeding rate and pressure of the cooling system.

High heat flux testing was performed using screening cycles of ~ 60-120 s before and after thermal cycling with 10 s loading and 10 s dwell time at a particular power density. The screening was used on the one hand to adjust the absorbed power density using water calorimetric measurements and on the other hand to determine the cool down performance of the loaded tiles via IR-thermography. This allowed the qualitative determination of preexisting or thermal fatigue induced defects.

The full loading histories of mock-up M-1_2 and M-2_2 are given in Table 1 and Table 2, respectively. Mock-up M-1_2 was tested on all 7 blocks at an absorbed power density of ~ 10 MW/m^2 for 769 cycles without obvious degradation. Due to an accidental loss of coolant pressure and therefore coolant flow in combination with an insufficient tilting of the component, electron loading was performed directly on the non-cooled Cu-tube causing melting and water leakage in at least two gaps between the blocks. However, cycling at 10 MW/m^2 caused no degradation of the surface quality (roughening, cracking), indicating a still high quality of the component before the accident. Due to the accidental failure of the component, no further analyses were performed.

Mock-up M-2_2 was preloaded on 2 blocks at 10 MW/m^2 for 700 cycles in the electron beam facility EMS-60 at SWIP, Chengdu, China, as shown in Fig. 1. In order to keep reference blocks and to allow for the investigation of intermediate stages, loading in JUDITH 1 was restricted to blocks 4-6 at 10 MW/m^2 and finally blocks 4 and 5 at 20 MW/m^2. During testing, the temperature evolution was monitored with a FLIR IR-camera SC-3000 and with two-color pyrometers from the company

Fig. 1.. Top view image of component M-2_2; exposure area on block 3 and 4 correspond to loading in the e-beam facility EMS-60 at 10 MW/m^2.

Table 1
Loading history for M-1_2.

# of cycles	power density [MW/m^2]	M-1_2: comments
1 / 1	5 / 10	screening
769	10	block 1 to 7 stop due to cooling system malfunction and component failure

Table 2
Loading history for M-2_2.

# of cycles	power density [MW/m^2]	M-2_2: comments
700	10	block 3 and 4, EMS-60
1 / 1	5 / 10	screening block 4 to 6
500	10	block 4 to 6
2	10	screening block 4 to 6
1 / 1 / 2	5 / 10 / 20	screening block 4 and 5
300	20	block 4 and 5
2	20	screening block 4 and 5
1	20	screening block 5
200	20	block 5
1	20	screening block 5

Maurer for two temperature ranges (550-1600°C: 10 MW/m^2; 1000-3500°C: 20 MW/m^2).

The final examination was performed using the IR-thermography facility SATIR at CEA-Cadarache to non-destructively determine, if existing, thermal fatigue induced damage formation and by performing metallographic analyses on various blocks perpendicular and parallel to the cooling tube.

3. Results and discussion

3.1. High heat flux testing

The emissivity calibration of the IR-camera by the two-color pyrometer was done on block 4 and 5 due to different surface morphology. The measured temperature values during cycling and the resulting respective emissivity for the IR-camera are plotted in Fig. 2 and Fig. 3, respectively. The initial emissivity variation between block 4 and 5 results from the initial exposure in the e-beam facility EMS-60 causing strong surface roughening and therefore an emissivity increase. The difference between the two blocks does not change significantly during cycling at 10 MW/m^2 indicating that no further surface degradation took place. However, during cycling at 20 MW/m^2 starting already after the very first cycle the emissivity difference between block 4 and 5 narrows significantly, which is related to the e-beam induced surface modification. This is caused by local thermal shock loading due to high power densities in the beam spot and scanning of the beam leading to thermal fatigue induced damage, i.e. surface roughening, shallow crack formation and subsequent erosion of small W-grains.

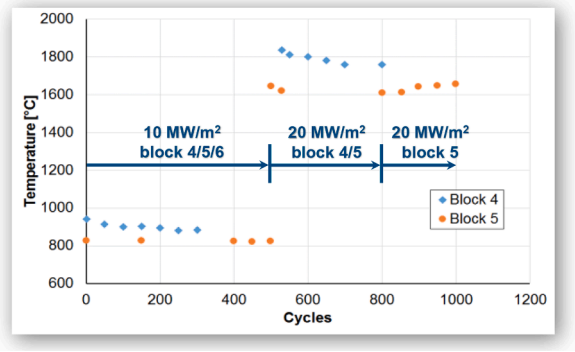

Fig. 2.. Pyrometer measurements during cycling.

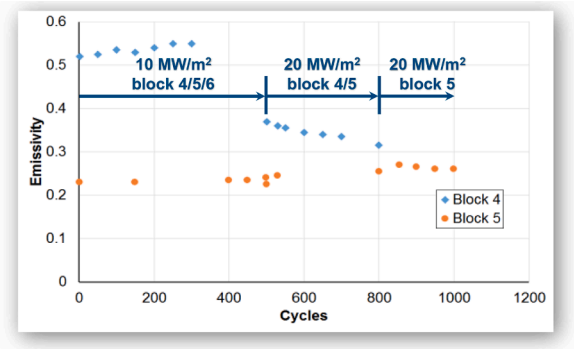

Fig. 3.. Emissivity evolution (IR-camera) during cycling.

The IR-images at the first and last cycle of each campaign are shown in Fig. 4 to Fig. 6. The before mentioned assimilation of emissivity is therein also highlighted in the IR-images after 300 cycles shown in Fig. 5. The images also indicate that no significant degradation of the component and in particular the interface took place as no local hot spot was observed. In addition, the cool down behavior for the most highly loaded block 5 before and after cycling at 20 MW/m^2 is plotted in Fig. 7 illustrating that no degradation of the cool down behavior took place which proves the high quality of the component and the intact heat transfer capability independent on the existence of the macro-crack on block 5 running parallel to the heat flow and therefore presenting no obstacle.

3.2. Post-mortem analyses

While for block 6, loaded only at 10 MW/m^2, no surface or bulk degradation could be determined, block 4 and 5 are characterized by the before mentioned e-beam induced surface degradation (Fig. 8) as well as recrystallization and thermally induced grain growth. In addition, block 5 experiences macro-crack formation down to a depth of 4-5 mm in the center of the block parallel to the cooling tube (Fig. 8), which is not visible from the top surface which might be due to the slight deflection of the crack in the vicinity of the top surface (see zoomed image in Fig. 8, bottom). This crack formation is described in literature [10-14]. While the fact that it has not yet reached the W/Cu interface leads to the conclusion that the crack is still growing and has just recently formed, the occurrence in literature is related to certain statistics. This means that, although in this case it is highly likely, it cannot be stated for sure that based on the lack of such a crack after 300 cycles on block 4 all components produced with this manufacturing technology and materials will survive 300 cycles at 20 MW/m^2 without macro-crack formation.

Figure 9

For the determination of the before mentioned recrystallization, hardness measurements were performed on tungsten for blocks 4 to 6 at the edge of the block with the largest distance to the cooling tube and from top to bottom. The results confirm, that no softening took place at

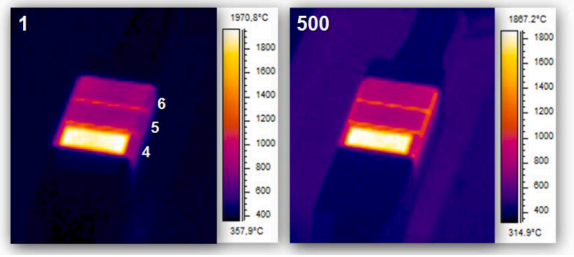

Fig. 4.. IR-images of M-2_2 during 1st and 500th cycle at 10 MW/m^2; emissivity adjusted for block 5.

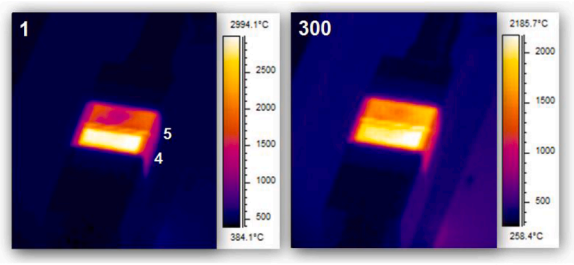

Fig. 5.. IR-images of M-2_2 during 1st and 300th cycle at 20 MW/m^2; emissivity adjusted for block 5.

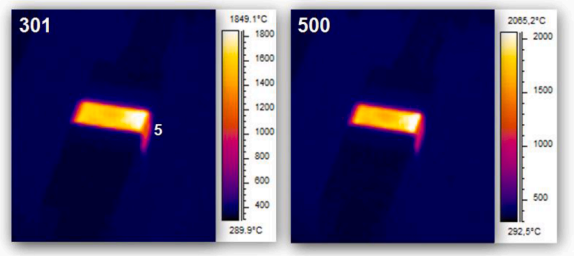

Fig. 6.. IR-images of M-2_2 during 301st and 500th cycle at 20 MW/m^2.

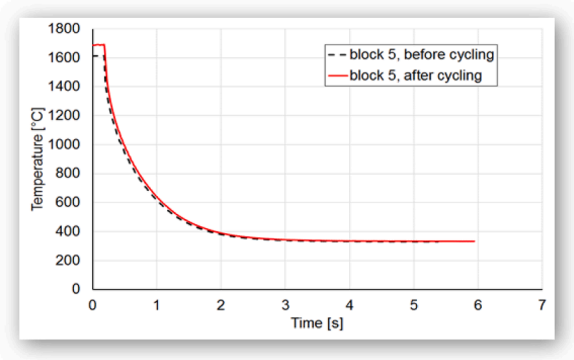

Fig. 7.. Cool down performance of block 5 after 500 cycles at 20 MW/m^2.

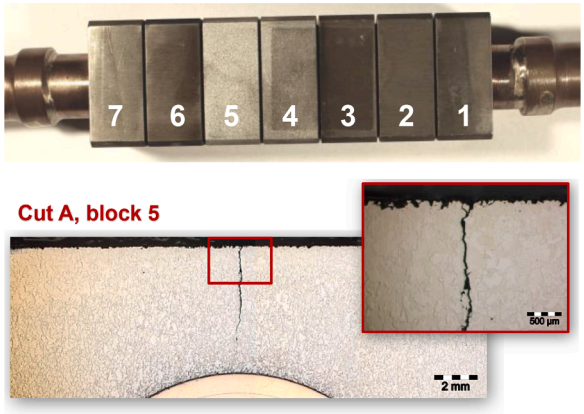

Fig. 8.. Surface view of the mock-up after high heat flux loading (top) and macroscopic crack formation in block 5 (bottom); surface roughening due to electron beam loading (local thermal shock induced thermal fatigue – similar to ELM-like loading effects shown in literature [15]).

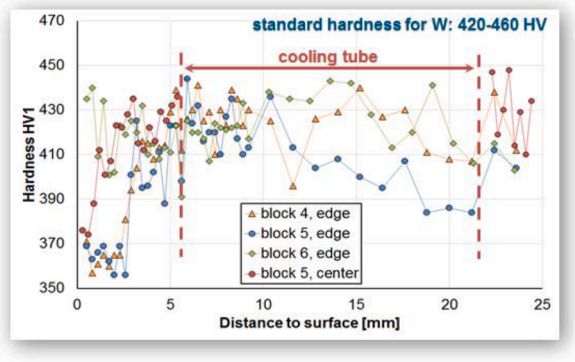

Fig. 9.. Vickers hardness of 3 different W-blocks perpendicular at the outer edge from the top surface to the backside and for block 5 in the near the macroscopic crack (see Fig. 8) from the top surface to the cooling tube interface.

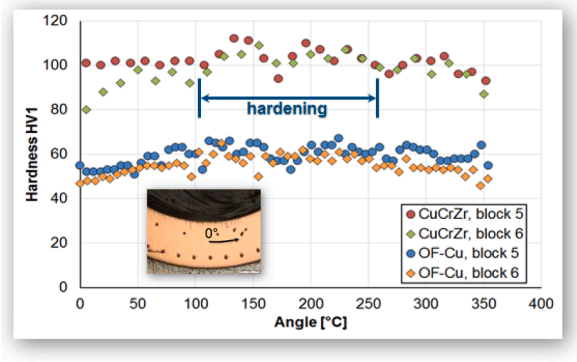

Fig. 10.. Vickers hardness of OF-Cu and CuCrZr in circumferential direction starting at the backside of the mock-up (closest to plasma facing top surface at 180°).

10 MW/m^2 (block 6) while at 20 MW/m^2 (block 4 & 5) are characterized by a fully softened material (~360 HV1) down to a depth of ~2.5 mm and a steep transition zone of ~0.5 mm to the average value of ~420 HV1. At the center of the loaded area and therefore at the shortest distance to the cooling tube, the affected area by recrystallization and grain growth is limited to ~0.6 mm. In general, the hardness measurements show locally a strong variation in particular in the non-heat affected zone, which might be related to the used load of 1 N testing only a limited volume and being therefore more sensitive to local inhomogeneity and the positioning of the indent.

Hardness measurements on OF-Cu and CuCrZr of block 5 and 6 were performed starting at the backside of the component and following the whole circumference. These show that in the top half close to the loaded area (90 – 270° in Fig. 10), best visible for CuCrZr, locally varying hardening took place that can be related to thermal stress induced deformations. Thereby, a local minimum was found at about the top center (180°), which is visible for block 5 in CuCrZr and OF-Cu, while for block 6 the minimum in OF-Cu was not observed.

However, the performed metallographic cross sections on block 4 to 6 perpendicular to the cooling tube do not indicate any macroscopic deformation in the cooling tube. Nevertheless, in cross sections on blocks 2 to 4 in the center of the blocks and parallel to the cooling tube (based on the cutting scheme this was not possible for blocks 4 to 6) it is shown, that CuCrZr shows an indication of local plastic deformation at the gap between block 3 and 4 (Fig. 11). This might be related to a local stress maximum caused by the high thermal loads on block 4, which needs to be studied and verified in further experiments by performing related metallographic analyses in those areas between two highly loaded blocks.

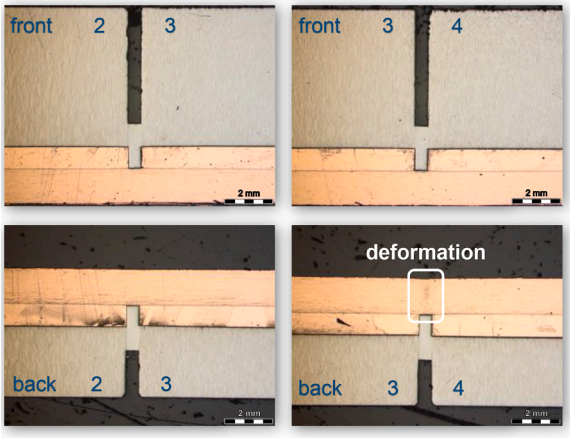

Fig. 11.. Cross sections of the area between adjacent blocks (2 to 4) at the front and backside.

4. Conclusion

Mock-up M-1_2 and M-2_2 were high heat flux tested and while the tests on M-1_2 stopped due to applying accidental conditions during cycling at 10 MW/m^2, three blocks of M-2_2 were tested up to a maximum of 500 cycles at 20 MW/m^2. While none of the loaded blocks failed during testing or showed degradation of the heat removal capacity, material modification and damage formation occurred:

- Surface roughening of loaded blocks due to e-beam scanning (local thermal shock induced thermal fatigue) – similarity with operational steady state and ELM-loading in a tokamak
- Macro-crack formation similar to those found in ITER mock-ups after 500 cycles at 20 MW/m^2
- Full softening of tungsten by recrystallization / grain growth down to ~2.5 mm (edge) and to ~0.6 mm (center) from top surface
- Hardening of CuCrZr and Cu due to plastic deformation in the top half with a minimum at the top center; effect visible already after testing at 10 MW/m^2
- Indications of deformation of CuCrZr between the two adjacent blocks 3 and 4 at the backside which might be related to loading of block 4 – further studies are necessary
- No degradation of the interfaces between W/Cu and Cu/CuCrZr

These promising results regarding the heat exhaust capability under thermal cycling up to 20 MW/m^2, obtained on W-monoblock small-scale mock-ups based on ITER-like technology, will enable a first qualification of the manufacturing process developed by the AT&M Chinese company. Finally, this outcome will lead afterwards to full-scale prototype manufacturing (so-called PFU - Plasma-Facing-Unit) successfully tested in WEST tokamak (2016-2020), followed by an industrial production (several hundreds of PFUs) for WEST and EAST divertor, both installed and tested in tokamak environment from 2021 [16].

CRediT authorship contribution statement

G. Pintsuk: Investigation, Formal analysis, Writing – original draft. **M. Missirlian:** Conceptualization, Supervision, Writing – review & editing. **G.-N. Luo:** . **Q. Li:** . **W. Wang:** . **D. Guilhem:** Project administration, Writing – review & editing. **J. Bucalossi:** .

Declaration of Competing Interest

The authors declare that they have no known competing financial interests or personal relationships that could have appeared to influence the work reported in this paper.

References

[1] A. Grosman, et al., The WEST programme: Minimizing technology and operational risks of a fullactively cooled tungsten divertor on ITER, Fusion Eng. Des. 88 (2013) 497–500.

[2] J. Bucalossi, et al., The WEST project: Testing ITER divertor high heat flux componenttechnology in a steady state tokamak environment, Fusion Eng. Des. 89 (2014) 907–912.

[3] M. Missirlian, et al., The WEST project: Current status of the ITER-like tungsten divertor, Fusion Eng. Des. 89 (2014) 1048–1053.

[4] R. Duwe, et al., The new electron beam facility for materials testing in hot cells, Fusion Technol. 27 (1995) 356–358.

[5] T. Hirai, et al., ITER tungsgen divertor design development and qualification program, Fusion Eng. Des. 88 (2013) 1798–1801.

[6] T. Hirai, et al., ITER full tungsten divertor qualification program and progress, Phys. Scr. T159 (2014), 014006 (5pp).

[7] P. Gavila, et al., High heat flux testing of EU tungsten monoblock mock-ups for the ITER divertor, Fusion Eng. Des. 98-99 (2015) 1305–1309.

[8] V.P. Budaev, et al., Nucl. Mater. Energy 25 (2020), 100816.

[9] V.P. Budaev, et al., Studying of in-vessel component materials under high power electron beam and steady-state plasma loads, Fusion Eng. Des. 164 (2021), 112335.

[10] G. Pintsuk, et al., Qualification and post-mortem characterization of tungsten mock-ups exposed to cyclic high heat flux loading, Fusion Eng. Des. 88 (2013) 1858–1861.

[11] G. Pintsuk, et al., Characterization of ITER tungsten qualification mock-ups exposed to high cyclic thermal loads, Fusion Eng. Des. 98-99 (2015) 1384–1388.

[12] S. Panayotis, et al., Self-castellation of tungsten monoblock under high heat flux loading and impact of material properties, Nucl. Mater. Energy 12 (2017) 200–204.

[13] S. Nogami, et al., Degradation of tungsten monoblock divertor under cyclic high heat flux loading, Fusion Eng. Des. 120 (2017) 49–60.

[14] M. Li, J.-H. You, Interpretation of the deep cracking phenomenon of tungsten monoblock targets observed in high-heat-flux fatigue tests at 20 MW/m2, Fusion Eng. Des. 101 (2015) 1–8.

[15] Th. Loewenhoff, et al., Impact of combined transient plasma/heat loads on tungsten performance below and above recrystallization temperature, Nucl. Fusion 55 (2015), 123004 (16pp).

[16] M. Firdaouss et al., First feedback during series fabrication of ITER like divertor tungsten components for the WEST tokamak, to be published in proceedings of the PFMC-18 (2021).